Fault Severity Estimation in 7-Phase Electrical Machines in a Noisy Environment

Lu Zhang, Claude Delpha, Demba Diallo

Fault Severity Estimation in 7-Phase Electrical Machines in a Noisy Environment

Lu ZHANG*, Claude DELPHA*, Demba DIALLO†

*Université Paris Saclay, CNRS, CentraleSupélec, Laboratoire des Signaux et Systèmes - Gif sur Yvette, France
†Université Paris Saclay, CentraleSupélec, CNRS, Group of Electrical Engineering of Paris - Gif sur Yvette, France

2023 IEEE 32nd International Symposium on Industrial Electronics (ISIE) | 979-8-3503-9971-4/23/$31.00 ©2023 IEEE | DOI: 10.1109/ISIE51358.2023.10227933

***Abstract*—This work proposes a method for estimating fault severity in the presence of noise using the measured currents for a 7-phase electrical machine. The method is based on analytical models in stationary reference frames and analysis of the DC and fundamental components in the four fictitious machines. The simulation results show that the estimation errors in the tertiary and homopolar machines are less noise-sensitive than in the principal machine, regardless of the fault severity level. On the other hand, if the fault significantly affects the magnitude of the currents (fault $> 10\%$), the estimation in the secondary machine is less sensitive to noise than in the main machine. If the fault results in a change in the mean value, the estimates using the main machine characteristics are less sensitive to noise. If the fault affects the phase shift, the estimates are less sensitive in the secondary machine than in the main one even if the noise is significant in the measurements.**

***Index Terms*—Fault severity estimation, 7-phase machines, Stationary frames, Frequency domain, Noisy environment**

NOMENCLATURE

θ	Electrical angle
ω	Angular frequency
I	RMS value of the phase current
$\triangle i_j$	Gain shift of j_{th} phase
ϕ_j	Phase shift of j_{th} phase
γ_j	Mean shift of j_{th} phase
φ	Natural phase shift of the 7-phase machine phases
i_0	Current in the Homopolar Machine
$i_{p\alpha}$	Current α axis in the Principal Machine
$i_{p\beta}$	Current β axis in the Principal Machine
$i_{s\alpha}$	Current α axis in the Secondary Machine
$i_{s\beta}$	Current β axis in the Secondary Machine
$i_{t\alpha}$	Current α axis in the Tertiary Machine
$i_{t\beta}$	Current β axis in the Tertiary Machine
y	Amplitude of noise-free harmonics
$\widetilde{y}$	Amplitude of noisy harmonics
x	Actual fault severity
$\hat{x}$	Estimated fault severity
ζ	Error criterion

I. INTRODUCTION

FAult Detection and Diagnosis (FDD), which can be decomposed into fault detection, isolation and estimation has become more and more attractive in the last decades in all industrial sectors [1]. In particular, attention has been paid to the monitoring of electrical machines which are at the heart of, for example, wind turbines or electric vehicles powertrain [2]. Although three-phase machines are still dominant, five-, seven-, nine-phase machines are increasingly being designed and used because of their inherent fault tolerance and power sharing capabilities [3]–[5]. This work focuses on monitoring a seven-phase electrical machine [6], [7], which is attractive in high power applications where reliability and availability are concerns. Usually, fault detection, isolation and estimation is based on the extraction and analysis of fault signatures or features from measured or estimated variables or parameters [2]. Those features can be extracted in time, frequency or time-frequency domain, depending on the fault types. In [8], the authors presented an approach in the time domain to detect and diagnose several faults in a three-phase electrical machine. In [9], the authors presented an analytical model of the currents flowing in a 7-phase machine, which can provide sensitive fault signatures in the time and frequency domains while considering that a fault effect leads to changes in mean, offset and phase of the electrical signal. Once the fault is detected and isolated, it is important for maintenance purposes or control reconfiguration to estimate the fault effect severity. The performance of the estimator depends on the accuracy of the model and the quality of the used measurements [10], [11]. Indeed, due to the increasing complexity of industrial systems, it is challenging to develop models, which are accurate in a wide operating range. Besides, measurements are very often polluted with nuisances due to switching devices and noise. This paper is a continuation of [9]. Most electrical or mechanical faults in electrical machines affect the spectrum or characteristics (amplitude, phase, mean value) of the currents flowing in the windings. This work does not deal with the control performance. Whatever the control structure, it assumes that the phase currents are affected by fault occurrence. The objectives are to detect the fault and estimate its severity with the highest performance. The main contributions are: (1) The development of analytical models in stationary frames of machine phase-currents when affected by faults that change their amplitude, phase or mean value; (2) The evaluation of the fault severity estimation performance for different noise levels.

The flowchart of the estimation procedure is displayed in

The authors would like to thank China Scholarship Council for funding.

Fig. 1. The rest of this paper is organized as follows: Section II (right side of the flowchart) describes how the theoretical relation between the fault severity and noise-free fault features is extracted. Section III (left side of the flowchart) presents how the fault severity is estimated from fault features under different noise levels. In section IV, the evaluation of the estimation performance in the different fictitious machines is provided based on the analysis of the normalized root mean square deviation. The conclusions are given in Section V.

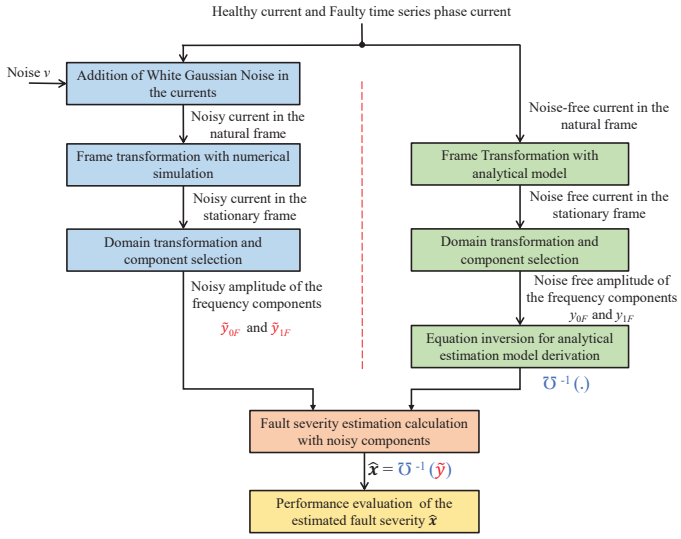

Fig. 1: Flowchart of fault estimation

II. Noise-free phase currents analysis

A. Description of frames

The 7-phase machine can be modeled in three representation spaces, expanding the conventional definition of space vector which is utilized for 3-phase systems [5], [9]:

- Natural frame: The variables for the 7 phases are denoted as x_1 to x_7.
- Stationary transformed (α, β) frame: it can be represented by a one-phase Homopolar Machine (HM) (variable is x_0) and three two-phase independent fictitious machines: a Principal Machine (PM) (variables are $x_{p\alpha}$ and $x_{p\beta}$), a Secondary Machine (SM) (variables are $x_{s\alpha}$ and $x_{s\beta}$), and a Tertiary Machine (TM) (variables are $x_{t\alpha}$ and $x_{t\beta}$).
- Synchronous transformed (d, q) frame: it is composed of a one-phase HM and three $d-q$ orthogonal coordinate fictitious machines.

In the following, the synchronous representation space is not considered. This study is limited to the analysis of the DC component $(0F)$ and/or fundamental component $(1F)$ of the phase currents. The healthy and faulty currents in the natural frame are expressed as follows, respectively [9]:

$$i_{j(j=1\ldots7)h} = I\sqrt{2}sin(\theta + (1-j)\varphi) \quad (1)$$

$$i_{j(j=1\ldots7)f} = I\sqrt{2}(1+\triangle i_j)sin(\theta + (1-j)\varphi + \phi_j) + \gamma_j \quad (2)$$

where, $\theta = \omega t$, ω is the angular frequency; t is the current time; $\varphi = \frac{2\pi}{7}$ is the natural phase shift multiple of the 7-phase machine; I represents the RMS value of the phase current; a gain fault, resulting in a modification of the current amplitude, can be denoted by $\triangle i_j$; a phase shift fault, which modifies the initial phase of the current, can be represented by ϕ_j; a bias in the mean value of the current can be represented by γ_j. The index j denotes the phase number; and h and f denote the healthy and faulty conditions, respectively.

Faults in a multi-electricity system can be categorized based on their location or origin, such as Generator Fault (fault occurs within a generator or other rotating machinery), Line Fault (fault occurs on a transmission or distribution line), Transformer Fault, Bus Fault (occurs within a bus or other electrical component that distributes power to multiple circuits) and so on. A fault can also be classified as symmetric or asymmetric according to whether it affects identically the phases. Usual faults include short-circuits, overload, ground fault, voltage sag or swell. Faults can interact, and each fault's impact depends on various factors, including its location, the equipment involved and the means of protection and control. For example, a short circuit can cause a significant increase in current, resulting in a change in amplitude (gain). However, a short circuit can cause a voltage drop or phase shift, mainly if the short circuit occurs near the end of a transmission line or sensitive equipment, which could result in a phase shift or mean value fault. Then, it can be assumed that no matter the fault type and evolution, the fault effect on the phase currents can be emulated with three main parameters, as described in the equation(2).

B. Analytical model for fault severity estimation

As discussed, the problem for a multi-dimensional system is to find the elementary independent 2-dimensional machines. The matrix derived in (3) can ensure the families of odd harmonics: $7n \pm 1$, $7n \pm 2$, and $7n \pm 3$, for PM, SM, and TM, respectively [5].

The analytical expressions of the phase currents in the stationary frames can be deduced by combining (2) and the Clarke transformation in (3). The detailed derivation process and results can be found in [9]. The general expressions of faulty currents under the three single faults are displayed in TABLE I to TABLE III.

TABLE I: Current under mean value fault

Analytical model, $\gamma_j \in (0, 1)$
$i_{p\alpha} = \sqrt{7} * I * sin\theta + \sqrt{\frac{2}{7}} * cos(j-1)\varphi * \gamma_j$
$i_{p\beta} = -\sqrt{7} * I * cos\theta - \sqrt{\frac{2}{7}} * sin(j-1)\varphi * \gamma_j$
$i_{s\alpha} = \sqrt{\frac{2}{7}} * cos(j-1)3\varphi * \gamma_j$
$i_{s\beta} = \sqrt{\frac{2}{7}} * sin(j-1)3\varphi * \gamma_j$
$i_{t\alpha} = \sqrt{\frac{2}{7}} * cos(j-1)2\varphi * \gamma_j$
$i_{t\beta} = \sqrt{\frac{2}{7}} * sin(j-1)2\varphi * \gamma_j$
$i_0 = \sqrt{\frac{1}{7}} * \gamma_j$

$$\begin{pmatrix} i_0 \\ i_{p\alpha} \\ i_{p\beta} \\ i_{t\alpha} \\ i_{t\beta} \\ i_{s\alpha} \\ i_{s\beta} \end{pmatrix} = \sqrt{\frac{2}{7}} \begin{pmatrix} \frac{1}{\sqrt{2}} & \frac{1}{\sqrt{2}} & \frac{1}{\sqrt{2}} & \frac{1}{\sqrt{2}} & \frac{1}{\sqrt{2}} & \frac{1}{\sqrt{2}} & \frac{1}{\sqrt{2}} \\ 1 & cos(\varphi) & cos(2\varphi) & cos(3\varphi) & cos(4\varphi) & cos(5\varphi) & cos(6\varphi) \\ 0 & sin(\varphi) & sin(2\varphi) & sin(3\varphi) & sin(4\varphi) & sin(5\varphi) & sin(6\varphi) \\ 1 & cos(2\varphi) & cos(4\varphi) & cos(6\varphi) & cos(8\varphi) & cos(10\varphi) & cos(12\varphi) \\ 0 & sin(2\varphi) & sin(4\varphi) & sin(6\varphi) & sin(8\varphi) & sin(10\varphi) & sin(12\varphi) \\ 1 & cos(3\varphi) & cos(6\varphi) & cos(9\varphi) & cos(12\varphi) & cos(15\varphi) & cos(18\varphi) \\ 0 & sin(3\varphi) & sin(6\varphi) & sin(9\varphi) & sin(12\varphi) & sin(15\varphi) & sin(18\varphi) \end{pmatrix} \begin{pmatrix} i_1 \\ i_2 \\ i_3 \\ i_4 \\ i_5 \\ i_6 \\ i_7 \end{pmatrix} \tag{3}$$

TABLE II: Current under gain fault

Analytical model, $\triangle i_j \in (0,1)$	
$i_{p\alpha} = \sqrt{\frac{1}{7}} * \sqrt{2 * \triangle i_j * (\triangle i_j + 7) * (1 + cos(j-1)2\varphi) + 49} * I * sin(\theta - \theta'_{p\alpha})$,	$tan\theta'_{p\alpha} = \frac{\triangle i_j * sin(j-1)2\varphi}{7 + \triangle i_j + \triangle i_j * cos(j-1)2\varphi}$
$i_{p\beta} = \sqrt{\frac{1}{7}} * \sqrt{2 * \triangle i_j * (\triangle i_j + 7) * (1 - cos(j-1)2\varphi) + 49} * I * sin(\theta - \theta'_{p\beta})$,	$tan\theta'_{p\beta} = \frac{7 + \triangle i_j - \triangle i_j * cos(j-1)2\varphi}{\triangle i_j * sin(j-1)2\varphi}$
$i_{s\alpha} = \sqrt{\frac{2}{7}} * \triangle i_j * \sqrt{1 + cos(j-1)6\varphi} * I * sin(\theta + \theta'_{s\alpha})$,	$tan\theta'_{s\alpha} = \frac{sin(j-1)2\varphi - sin(j-1)4\varphi}{cos(j-1)2\varphi + cos(j-1)4\varphi}$
$i_{s\beta} = \sqrt{\frac{2}{7}} * \triangle i_j * \sqrt{1 - cos(j-1)6\varphi} * I * sin(\theta - \theta'_{s\beta})$,	$tan\theta'_{s\beta} = \frac{cos(j-1)2\varphi - cos(j-1)4\varphi}{sin(j-1)2\varphi + sin(j-1)4\varphi}$
$i_{t\alpha} = \sqrt{\frac{2}{7}} * \triangle i_j * \sqrt{1 + cos(j-1)4\varphi} * I * sin(\theta + \theta'_{t\alpha})$,	$tan\theta'_{t\alpha} = \frac{sin(j-1)\varphi - sin(j-1)3\varphi}{cos(j-1)\varphi + cos(j-1)3\varphi}$
$i_{t\beta} = \sqrt{\frac{2}{7}} * \triangle i_j * \sqrt{1 - cos(j-1)4\varphi} * I * sin(\theta + \theta'_{t\beta})$,	$tan\theta'_{t\beta} = \frac{cos(j-1)\varphi - cos(j-1)3\varphi}{sin(j-1)\varphi + sin(j-1)3\varphi}$
$i_0 = \sqrt{\frac{2}{7}} * \triangle i_j * I * sin(\theta - (j-1)\varphi)$	

TABLE III: Current under phase shift fault

Analytical model, $\phi_j \in (0, \varphi)$
$i_{p\alpha} = \sqrt{\frac{1}{7}} * \sqrt{39 + 10 * cos\phi_j - 10 * cos(j-1)2\varphi + 12 * cos(\phi_j - (j-1)2\varphi) - 2 * cos(\phi_j + (j-1)2\varphi)} * I * sin(\theta + \theta'_{p\alpha})$,
$tan\theta'_{p\alpha} = \frac{sin\phi_j + sin(j-1)2\varphi + sin(\phi_j - (j-1)2\varphi)}{6 + cos\phi_j - cos(j-1)2\varphi + cos(\phi_j - (j-1)2\varphi)}$
$i_{p\beta} = \sqrt{\frac{1}{7}} * \sqrt{39 + 10 * cos\phi_j + 10 * cos(j-1)2\varphi - 12 * cos(\phi_j - (j-1)2\varphi) + 2 * cos(\phi_j + (j-1)2\varphi)} * I * sin(\theta - \theta'_{p\beta})$,
$tan\theta'_{p\beta} = \frac{6 + cos\phi_j + cos(j-1)2\varphi - cos(\phi_j - (j-1)2\varphi)}{sin\phi_j - sin(j-1)2\varphi - sin(\phi_j - (j-1)2\varphi)}$
$i_{s\alpha} = \sqrt{\frac{1}{7}} * \sqrt{4 * (1 + cos(j-1)6\varphi - cos\phi_j) - 2 * (cos(\phi_j - (j-1)6\varphi) + cos(\phi_j + (j-1)6\varphi))} * I * sin(\theta + \theta'_{s\alpha})$,
$tan\theta'_{s\alpha} = \frac{sin(\phi_j + (j-1)2\varphi) + sin(\phi_j - (j-1)4\varphi) - sin(j-1)2\varphi + sin(j-1)4\varphi}{cos(\phi_j + (j-1)2\varphi) + cos(\phi_j - (j-1)4\varphi) - cos(j-1)2\varphi - cos(j-1)4\varphi}$
$i_{s\beta} = \sqrt{\frac{1}{7}} * \sqrt{4 * (1 - cos(j-1)6\varphi - cos\phi_j) + 2 * (cos(\phi_j - (j-1)6\varphi) + cos(\phi_j + (j-1)6\varphi))} * I * sin(\theta - \theta'_{s\beta})$,
$tan\theta'_{s\beta} = \frac{cos(\phi_j + (j-1)2\varphi) - cos(\phi_j - (j-1)4\varphi) - cos(j-1)2\varphi + cos(j-1)4\varphi}{sin(\phi_j + (j-1)2\varphi) - sin(\phi_j - (j-1)4\varphi) - sin(j-1)2\varphi - sin(j-1)4\varphi}$
$i_{t\alpha} = \sqrt{\frac{1}{7}} * \sqrt{4 * (1 + cos(j-1)4\varphi - cos\phi_j) - 2 * (cos(\phi_j - (j-1)4\varphi) + cos(\phi_j + (j-1)4\varphi))} * I * sin(\theta + \theta'_{t\alpha})$,
$tan\theta'_{t\alpha} = \frac{sin(\phi_j + (j-1)\varphi) + sin(\phi_j - (j-1)3\varphi) - sin(j-1)\varphi + sin(j-1)3\varphi}{cos(\phi_j + (j-1)\varphi) + cos(\phi_j - (j-1)3\varphi) - cos(j-1)\varphi - cos(j-1)3\varphi}$
$i_{t\beta} = \sqrt{\frac{1}{7}} * \sqrt{4 * (1 - cos(j-1)4\varphi - cos\phi_j) + 2 * (cos(\phi_j - (j-1)4\varphi) + cos(\phi_j + (j-1)4\varphi))} * I * sin(\theta - \theta'_{t\beta})$,
$tan\theta'_{t\beta} = \frac{cos(\phi_j + (j-1)\varphi) - cos(\phi_j - (j-1)3\varphi) - cos(j-1)\varphi + cos(j-1)3\varphi}{sin(\phi_j + (j-1)\varphi) - sin(\phi_j - (j-1)3\varphi) - sin(j-1)\varphi - sin(j-1)3\varphi}$
$i_0 = 2 * \sqrt{\frac{1}{7}} * \sqrt{1 - cos\phi_j} * I * sin(\theta + \theta'_0)$, $\quad tan\theta'_0 = \frac{sin(\phi_j - (j-1)\varphi) + sin(j-1)\varphi}{cos(\phi_j - (j-1)\varphi) - cos(j-1)\varphi}$

Under healthy conditions, there is no current flowing in the SM, TM, and HM. However, when the system is faulty, new components and/or frequency distortions will appear in the actual phase currents [9]. The frequency analysis is summarized in TABLE IV. It can be noticed that the spectrum of the faulty current in the stationary frames includes DC ($0F$) and/or fundamental component ($1F$). It can be observed that only the mean value fault induces the presence of DC ($0F$) component in the four fictitious machines [9].

For gain, phase shift, and mean value faults, the fault severity $x \in [0,1]$ corresponds to the modification of parameters $\triangle i_j$, ϕ_j and γ_j, respectively. The relations between the amplitude of the components y for $0F$ and $1F$ and the fault severity x can be expressed by a function $y = \mho(x)$, as it can be seen in TABLE V to TABLE VII. These functions, retrieved under noise-free conditions are then used to estimate the fault parameter from the noisy fault features (Fig. 1).

TABLE IV: Fault frequencies in the stationary frames

Case	Current		Harmonic $0F$	Harmonic $1F$	Case	Current		Harmonic $0F$	Harmonic $1F$
H	PM	$i_{p\alpha}$		×	G	PM	$i_{p\alpha}$		×
		$i_{p\beta}$		×			$i_{p\beta}$		×
	SM	$i_{s\alpha}$				SM	$i_{s\alpha}$		×
		$i_{s\beta}$					$i_{s\beta}$		×(1)
	TM	$i_{t\alpha}$				TM	$i_{t\alpha}$		×
		$i_{t\beta}$					$i_{t\beta}$		×(1)
	HM	i_0				HM	i_0		×
PS	PM	$i_{p\alpha}$		×	MV	PM	$i_{p\alpha}$	×	×
		$i_{p\beta}$		×			$i_{p\beta}$	×(2)	×
	SM	$i_{s\alpha}$		×		SM	$i_{s\alpha}$	×	
		$i_{s\beta}$		×(1)			$i_{s\beta}$	×(3)	
	TM	$i_{t\alpha}$		×		TM	$i_{t\alpha}$	×	
		$i_{t\beta}$		×(1)			$i_{t\beta}$	×(3)	
	HM	i_0		×		HM	i_0	×	

H: healthy; G: gain fault; PS: phase shift fault; MV: mean value fault.
(1) For phase 1, no $1F$ component for $i_{s\beta}$ and $i_{t\beta}$.
(2) For phase 1, no $0F$ component for $i_{p\beta}$.
(3) For phase 1, no $0F$ component for $i_{s\beta}$ and $i_{t\beta}$.

TABLE V: Evolution of fault severity under mean value fault

i	$0F$	$1F$
$i_{p\alpha}$	$y = kx, \quad k = 2 * \sqrt{\frac{1}{7}} * \lvert cos(j-1)\varphi) \rvert * I$	$y = \frac{\sqrt{7}}{2} * I$
$i_{p\beta}$	$y = kx, \quad k = 2 * \sqrt{\frac{1}{7}} * \lvert sin(j-1)\varphi) \rvert * I$	$y = \frac{\sqrt{7}}{2} * I$
$i_{s\alpha}$	$y = kx, \quad k = 2 * \sqrt{\frac{1}{7}} * \lvert cos(j-1)3\varphi) \rvert * I$	/
$i_{s\beta}$	$y = kx, \quad k = 2 * \sqrt{\frac{1}{7}} * \lvert sin(j-1)3\varphi) \rvert * I$	/
$i_{t\alpha}$	$y = kx, \quad k = 2 * \sqrt{\frac{1}{7}} * \lvert cos(j-1)2\varphi) \rvert * I$	/
$i_{t\beta}$	$y = kx, \quad k = 2 * \sqrt{\frac{1}{7}} * \lvert sin(j-1)2\varphi) \rvert * I$	/
i_0	$y = kx, \quad k = \sqrt{\frac{2}{7}} * I$	/

TABLE VI: Evolution of fault severity under gain fault

i	$0F$	$1F$
$i_{p\alpha}$	/	$y = \frac{1}{2} * \sqrt{\frac{1}{7}} * \sqrt{2x(x+7)(1+cos(j-1)2\varphi)+49} * I$
$i_{p\beta}$	/	$y = \frac{1}{2} * \sqrt{\frac{1}{7}} * \sqrt{2x(x+7)(1-cos(j-1)2\varphi)+49} * I$
$i_{s\alpha}$	/	$y = kx, \quad k = \frac{1}{2} * \sqrt{\frac{2}{7}} * \sqrt{1+cos(j-1)6\varphi} * I$
$i_{s\beta}$	/	$y = kx, \quad k = \frac{1}{2} * \sqrt{\frac{2}{7}} * \sqrt{1-cos(j-1)6\varphi} * I$
$i_{t\alpha}$	/	$y = kx, \quad k = \frac{1}{2} * \sqrt{\frac{2}{7}} * \sqrt{1+cos(j-1)4\varphi} * I$
$i_{t\beta}$	/	$y = kx, \quad k = \frac{1}{2} * \sqrt{\frac{2}{7}} * \sqrt{1-cos(j-1)4\varphi} * I$
i_0	/	$y = kx, \quad k = \frac{1}{2} * \sqrt{\frac{2}{7}} * I$

III. Noisy phase currents analysis

A. Settings for the numerical model

A white Gaussian noise is added to the phase currents to simulate realistic measurements. To define the noise level, the Signal to Noise Ratio (SNR) is considered. As reminder $SNR = 10 * \log_{10} \frac{\sigma_s^2}{\sigma_\upsilon^2}$, where, σ_s^2 is the variance of the signal, and σ_υ^2 is the variance of the Gaussian distributed noise $\upsilon \sim \mathcal{N}(0, \sigma_\upsilon^2)$. The following simulation studies are coded in MATLAB 2021a, and are carried out on a personal computer with an Intel Core i7 vPro 10th generation processor and 32 GB of memory. In the following, the SNR is set to 20, 15, 10 and 5 dB, respectively. When the SNR decreases, the noise level increases. The fault levels are set to [5% to 30%] for the three cases: gain fault varies from 0.05 to 0.3; phase shift varies from 0.05φ to 0.3φ, and mean value fault varies from $0.05I\sqrt{2}$ to $0.3I\sqrt{2}$. Two hundred simulations are run for the healthy conditions, but also each faulty severity case and each noise level (three single fault types, and four SNR values). Without losing generality, the RMS value of the phase current is assumed to be 4A, and only the results for the faults in the fourth phase of the machine are presented.

B. Estimated fault severity

The fault severity estimation under noisy conditions is done in two steps: (i) under noise-free conditions, the function $\mho^{-1}(.)$ is obtained through the analytical models, from the fault features (amplitude of DC and $1F$ components) and actual fault severity. (ii), the fault severity is estimated with the fault features extracted from noisy measurements such as $\hat{x} = \mho^{-1}(\widetilde{y})$.

Fig. 2 represents the estimated fault severity versus the actual one when using $i_{p\alpha}$ under gain fault case when SNR equals to 20 and 5 dB respectively. For each severity, the simulation is repeated 200 times. The red dots are the average values, which are close to the actual fault level. However, we can observe an increase of the variance with the noise level. This is confirmed with the histograms displayed in Fig. 3, which show that the estimation follows, as expected, the Gaussian distribution. The same computations are done for all the phase current components of the four fictitious machines in the stationary representation frames.

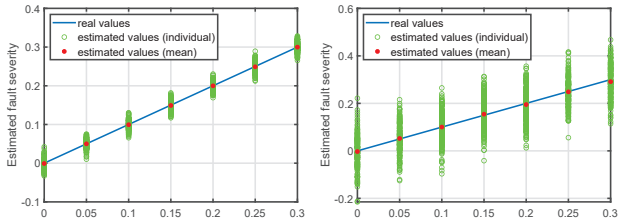

(a) SNR = 20 dB (b) SNR = 5 dB

Fig. 2: Fault severity estimation with $i_{p\alpha}$ under gain fault

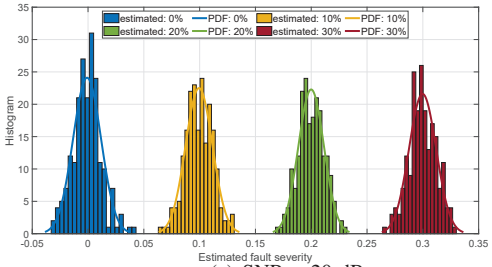

(a) SNR = 20 dB

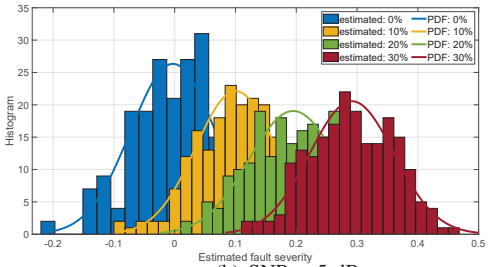

(b) SNR = 5 dB

Fig. 3: Histograms with $i_{p\alpha}$ under gain fault

IV. Fault estimation performance evaluation

To evaluate the fault estimation performance, first the relative error is defined as $\zeta = \frac{x-\hat{x}}{x}$, where the actual fault severity is x and the estimated one $\hat{x}$. Its averaged value (for the 200 simulations) is displayed in Fig. 4 to Fig. 6 for the three single faults and the considered current component in the stationary frame. It can be concluded that: (1) For the same SNR level, the average error becomes negligible when the fault severity increases; (2) For the same fault severity, the noise degrades the estimation; (3) The noise effect is higher for gain and phase shift fault than mean value fault; (4) The component

TABLE VII: Evolution of fault severity under phase shift fault

i	$0F$	$1F$
$i_{p\alpha}$	/	$y = \frac{1}{2} * \sqrt{\frac{1}{7}} * \sqrt{39 + 10 * cos\varphi x - 10 * cos(j-1)2\varphi + 12 * cos(\varphi x - (j-1)2\varphi) - 2 * cos(\varphi x + (j-1)2\varphi)} * I$
$i_{p\beta}$	/	$y = \frac{1}{2} * \sqrt{\frac{1}{7}} * \sqrt{39 + 10 * cos\varphi x + 10 * cos(j-1)2\varphi - 12 * cos(\varphi x - (j-1)2\varphi) + 2 * cos(\varphi x + (j-1)2\varphi)} * I$
$i_{s\alpha}$	/	$y = \frac{1}{2} * \sqrt{\frac{1}{7}} * \sqrt{4 * (1 + cos(j-1)6\varphi - cos\varphi x) - 2 * (cos(\varphi x - (j-1)6\varphi) + cos(\varphi x + (j-1)6\varphi))} * I$
$i_{s\beta}$	/	$y = \frac{1}{2} * \sqrt{\frac{1}{7}} * \sqrt{4 * (1 - cos(j-1)6\varphi - cos\varphi x) + 2 * (cos(\varphi x - (j-1)6\varphi) + cos(\varphi x + (j-1)6\varphi))} * I$
$i_{t\alpha}$	/	$y = \frac{1}{2} * \sqrt{\frac{1}{7}} * \sqrt{4 * (1 + cos(j-1)4\varphi - cos\varphi x) - 2 * (cos(\varphi x - (j-1)4\varphi) + cos(\varphi x + (j-1)4\varphi))} * I$
$i_{t\beta}$	/	$y = \frac{1}{2} * \sqrt{\frac{1}{7}} * \sqrt{4 * (1 - cos(j-1)4\varphi - cos\varphi x) + 2 * (cos(\varphi x - (j-1)4\varphi) + cos(\varphi x + (j-1)4\varphi))} * I$
i_0	/	$y = \sqrt{\frac{1}{7}} * \sqrt{1 - cos\varphi x} * I$

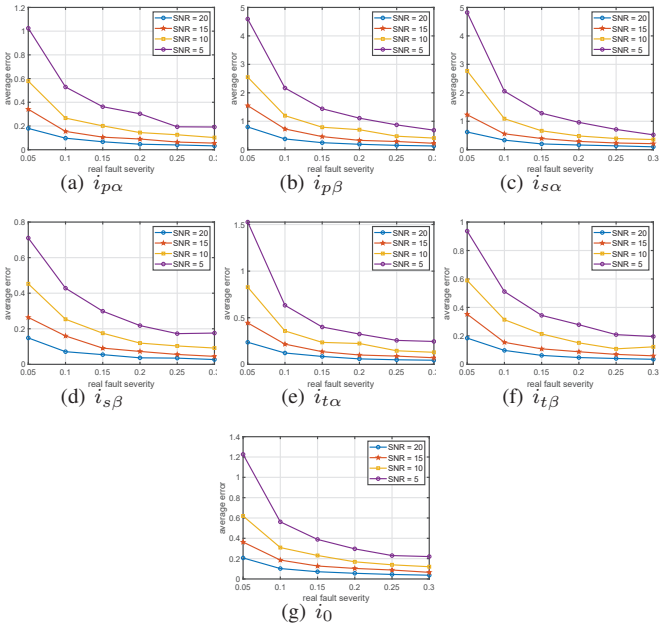

(a) $i_{p\alpha}$ (b) $i_{p\beta}$ (c) $i_{s\alpha}$ (d) $i_{s\beta}$ (e) $i_{t\alpha}$ (f) $i_{t\beta}$ (g) i_0

Fig. 4: Average fault estimation error under gain fault

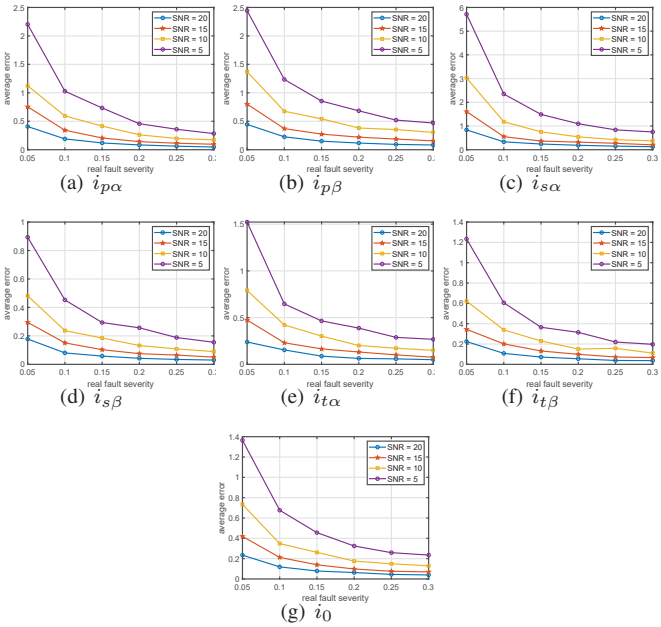

(a) $i_{p\alpha}$ (b) $i_{p\beta}$ (c) $i_{s\alpha}$ (d) $i_{s\beta}$ (e) $i_{t\alpha}$ (f) $i_{t\beta}$ (g) i_0

Fig. 5: Average fault estimation error under phase shift fault

$i_{s\alpha}$ is the most sensitive to the noise for all fault types; (5) For gain fault, $i_{p\beta}$ and $i_{s\alpha}$ are the most sensitive to the noise.

Hereafter, we analyze the fault estimation error in the four different fictitious machines. Therefore, the Normalized Root Mean Square Deviation (NRMSD) is introduced:

$$NRMSD = \sqrt{\frac{\sum_{n=1}^{N}(\hat{x}_n - x)^2}{N}}/\mu_{\hat{x}} \tag{4}$$

where, $\hat{x}_n$ represents the estimated fault severity; x denotes the real fault severity; $\mu_{\hat{x}}$ is the average estimated fault severity; N is the number of estimated values ($N = 200$). The NRMSD values for the estimation using the α and β axis information can be considered simultaneously, so the NRMSD value for each fictitious machine PM, SM, TM, and HM can be expressed as follows, respectively:

$$\|NRMSD_P\| = \sqrt{NRMSD_{p_\alpha}^2 + NRMSD_{p_\beta}^2} \tag{5}$$

$$\|NRMSD_S\| = \sqrt{NRMSD_{s_\alpha}^2 + NRMSD_{s_\beta}^2} \tag{6}$$

$$\|NRMSD_T\| = \sqrt{NRMSD_{t_\alpha}^2 + NRMSD_{t_\beta}^2} \tag{7}$$

$$\|NRMSD_H\| = NRMSD_h \tag{8}$$

In order to compare the estimation efficiency between the fictitious machines, if we consider the principal machine as the reference, we can compute the NRMSD ratio R such as:

$$R_{s/p} = \|NRMSD_S\|/\|NRMSD_P\| \tag{9}$$

$$R_{t/p} = \|NRMSD_T\|/\|NRMSD_P\| \tag{10}$$

$$R_{h/p} = \|NRMSD_H\|/\|NRMSD_P\| \tag{11}$$

The results are displayed in Fig.s 7 to 10. It can be concluded that: (1) For gain fault, the estimation is more sensitive to the noise in the PM. (2) For phase shift fault, whatever the fault level, the estimation is less sensitive to the noise in the tertiary and homopolar machines. Under low noise level conditions, the PM is more suitable for fault estimation than the SM, particularly for high fault severities. (3) For mean value fault, the PM is less sensitive to the noise than the SM for fault estimation. The tertiary and homopolar ones exhibit the highest robustness. (4) We can notice that the fault estimation error ratio is almost constant for all fault types and severities.

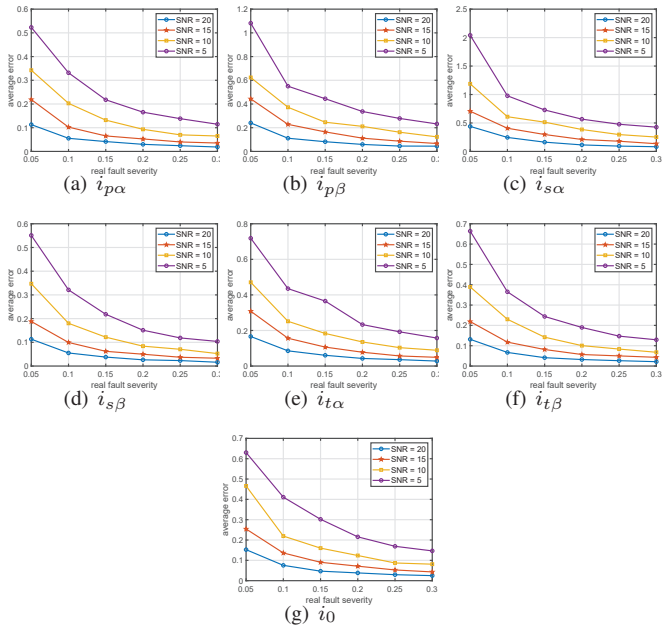

(a) $i_{p\alpha}$ (b) $i_{p\beta}$ (c) $i_{s\alpha}$

(d) $i_{s\beta}$ (e) $i_{t\alpha}$ (f) $i_{t\beta}$

(g) i_0

Fig. 6: Average fault estimation error under mean value fault

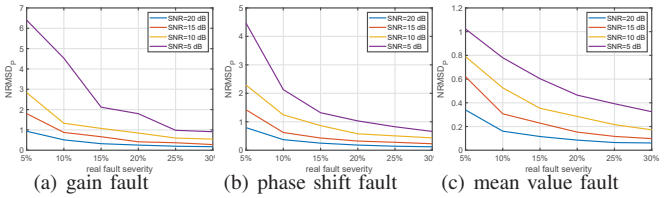

(a) gain fault (b) phase shift fault (c) mean value fault

Fig. 7: NRMSD with the PM

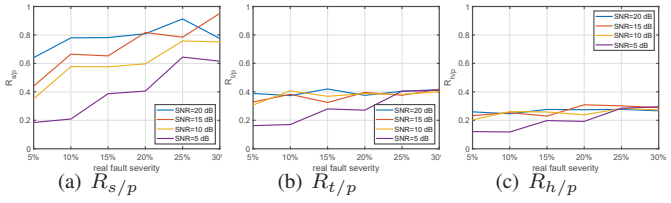

(a) $R_{s/p}$ (b) $R_{t/p}$ (c) $R_{h/p}$

Fig. 8: Estimation errors ratio for gain fault

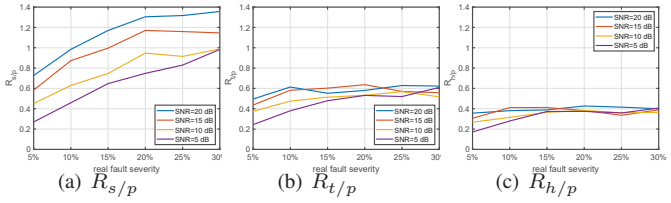

(a) $R_{s/p}$ (b) $R_{t/p}$ (c) $R_{h/p}$

Fig. 9: Estimation errors ratio for phase shift fault

V. Conclusion

This paper evaluates the performance of a fault estimator to the fault severity and noise levels. The case study is a seven-phase electrical machine for which it is assumed that most of the faults have an impact on the magnitude, phase or mean value of the phase currents. An analytical

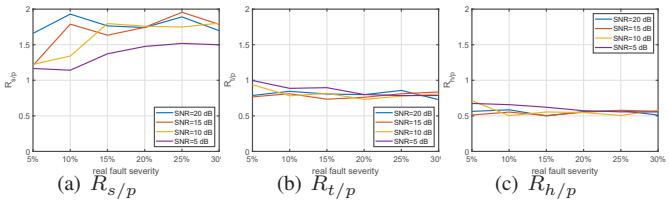

(a) $R_{s/p}$ (b) $R_{t/p}$ (c) $R_{h/p}$

Fig. 10: Estimation errors for mean value fault

model is developed from which the relations between the fault severity and the fault features (DC and $1F$ components) are extracted under noise-free conditions. These relations are then used to estimate the fault severity from noisy features. The relative error is used to evaluate the estimation performance. From the Monte-Carlo simulations, the results showed that for different fault severities (0 to 30%), and different noise levels (20 to 5dB), the current components of the tertiary and homopolar fictitious machines, in the stationary representation space, are the most robust to the nuisances. Future works will further analyze the estimation robustness performance, and its application to experimental data. The estimation in the synchronous representation spaces will also be investigated because the current components are also usually available within the electrical drive.

References

[1] M. Basseville and I. V. Nikiforov, *Detection of abrupt changes: theory and application*. prentice Hall Englewood Cliffs, 1993, vol. 104.

[2] M. Benbouzid, Ed., *Signal Processing for Fault Detection and Diagnosis in Electric Machines and Systems*, ser. Energy Engineering. Institution of Engineering and Technology, 2020.

[3] E. Ward and H. Härer, "Preliminary investigation of an invertor-fed 5-phase induction motor," in *Proceedings of the Institution of Electrical Engineers*, vol. 116, no. 6. IET, 1969, pp. 980–984.

[4] D. Diallo and C. Delpha, "Current-based analytical model derivation to analyse fault effects in 5-phase PMSM," in *IEEE International Power Electronics and Application Conference and Exposition (PEAC)*. IEEE, 2018, pp. 1–6.

[5] E. Semail, A. Bouscayrol, and J.-P. Hautier, "Vectorial formalism for analysis and design of polyphase synchronous machines," *The European physical journal-applied physics*, vol. 22, no. 3, pp. 207–220, 2003.

[6] M. Thavot, A. Iqbal, M. Saleh, and A. Kalam, "Modeling of a seven-phase series-connected three-motor drive system," in *IEEE GCC Conference and Exhibition (GCC)*. IEEE, 2013, pp. 142–147.

[7] D. Zhang, B. Xu, H. Yang, and P. Zhu, "Simulation analysis of SVPWM based on seven-phase permanent magnet synchronous motor," in *International Conference on Control, Automation and Information Sciences (ICCAIS)*. IEEE, 2017, pp. 251–256.

[8] C. Delpha, D. Diallo, H. Al Samrout, and N. Moubayed, "Multiple incipient fault diagnosis in three-phase electrical systems using multivariate statistical signal processing," *Engineering Applications of Artificial Intelligence*, vol. 73, pp. 68–79, 2018.

[9] L. Zhang, C. Delpha, and D. Diallo, "Current-based analytical model for fault detection and diagnosis in 7-phase machines," in *IEEE Industrial Electronics Society Conference (IECON)*, 2022, pp. 1–6.

[10] S. M. Kay, *Fundamentals of statistical signal processing: estimation theory*. Prentice-Hall, Inc., 1993.

[11] J. Stoustrup and H. H. Niemann, "Fault estimation - a standard problem approach," *International Journal of Robust and Nonlinear Control: IFAC-Affiliated Journal*, vol. 12, no. 8, pp. 649–673, 2002.